Applied Surface Science 455 (2018) 276–282

Contents lists available at ScienceDirect

Applied Surface Science

journal homepage: www.elsevier.com/locate/apsusc

Full Length Article

Hydrothermal synthesis and controlled growth of hierarchical 3D flower-like MoS_2 nanospheres assisted with CTAB and their NO_2 gas sensing properties

Yajie Zhang[a], Wen Zeng[a,*], Yanqiong Li[b]

[a] College of Materials Science and Engineering, Chongqing University, Chongqing 400030, China
[b] School of Electronic and Electrical Engineering, Chongqing University of Arts and Sciences, Chongqing 400030, China

ARTICLE INFO

Keywords:
Nanostructures
MoS_2
Hydrothermal
Gas sensors
Formation mechanism

ABSTRACT

Hierarchical 3D flower-like MoS_2 nanospheres with the diameter of about 300 nm were successfully synthesized via a facile hydrothermal process assisted with CTAB. And we found that CTAB played a vital role on the formation of MoS_2 architectures. As the concentration of CTAB increasing, MoS_2 nanopowders with sheet-like, flower-like, large size spherical morphologies were synthesized. And particle sizes of synthesized powders also increased. The optimum concentration of CTAB for the well-defined 3D hierarchical spherical morphology of MoS_2 was 6 g/L. In addition, a feasible formation mechanism of the morphology evolution was put forward in detail on the basis of the experimental results. The gas–sensing properties of flower-like MoS_2 nanospheres were tested. The result indicated that the sensor exhibited high response and selectivity towards NO_2, which may be related to the open and well-defined structures and the abundant micro reaction rooms assembled by ultrathin nanosheets.

1. Introduction

With the development of industry and technology, Atmospheric pollution has become a critical problem. Nitrogen dioxide (NO_2), as a typical air pollutant, is a reddish-brown and one of the toxic gases with pungent smell. It mainly results from automobile exhaust emission, automobile industries, electricity generation, fossil fuel combustion, industrial processes, waste disposal, and fires [1]. NO_2 can produce ground-level ozone in the atmospheric reactions. Additionally, it is also a main source of acid rain, photochemical smog and pollution haze [2]. According to the recent studies that NO_2 harms human health even at extremely low concentrations. Human exposure to NO_2 gas with a concentration of 3 ppm can give rise to irritation to the throat, and respiratory system, while increasing concentrations can cause more severe problems, including respiratory diseases, pulmonary edema, and even death [3]. Therefore, the development of simple and cost-effective chemical sensors with excellent performance for fast and reliable detection of NO_2 gas, plays a crucial role for environmental protection, human health, biomedicine, and industrial production.

In the past few years, much efforts have been put forth to develop a high sensitive, fast response, simplicity of fabrication and low cost sensor. Among gas-sensing materials, molybdenum disulfide (MoS_2) with its unique n-type semiconductor characteristics and low price has more potential value in the field of gas sensor application because it exhibits unique mechanical, optical and electrical properties [4–6]. MoS_2 has layered structure composing of S–Mo–S three layers bound by the weak Van der Waals forces, resulting in materials with fascinating properties [7]. More importantly, MoS_2 possesses a tunable band gap that depends on the number of MoS_2 layers. The band gap of bulk MoS_2 is 1.2 eV. Dramatically, for two-dimensional single-layer sheets the band gap becomes 1.8 eV [8–10]. This characteristic plays a critical role in improving its sensing performances [10]. The semiconducting behavior can improve sensing performance owing to modulating the transport characteristics with exposure to light or gate bias. In addition, hierarchical MoS_2 nanostructures using lower dimension nanocrystals as the building blocks attract more attention due to their more sensitive electronic properties, their less gas diffusion length, higher mobility, and relatively larger surface-to-volume ratio than the agglomerated nanoparticles [11]. Hence, 3D hierarchical MoS_2 is considered as the most promising alternative candidates for the next-generation gas sensing devices [12].

In this study, novel hierarchical 3D flower-like MoS_2 nanospheres with diameter of about 300 nm were successfully synthesized via a facile hydrothermal process assisted with CTAB. In order to find the

* Corresponding author.
E-mail address: wenzeng@cqu.edu.cn (W. Zeng).

https://doi.org/10.1016/j.apsusc.2018.05.224
Received 23 April 2018; Received in revised form 22 May 2018; Accepted 29 May 2018
Available online 30 May 2018
0169-4332/

optimum concentration of CTAB for the preparation of well-defined 3D hierarchical spherical morphology of MoS_2, the effects of CTAB concentration on the nanostructures and morphologies of MoS_2 were investigated. Surprisingly, the morphologies of final obtained MoS_2 can be tailored by varying the concentration of CTAB. In addition, a feasible formation mechanism of the morphology evolution was put forward in detail on the basis of the experimental results. The gas-sensing properties of the hierarchical 3D flower-like MoS_2 nanospheres were also investigated. As a result, the sensor exhibited remarkable sensing performance toward Nitrogen dioxide, especially its fast response, high sensitivity, better selectivity and stability.

2. Experimental

2.1. Sample preparation

All the chemicals were of analytic purity and used directly without any further purification. In a typical synthesis, 1 g of $Na_2MoO_4{\cdot}2H_2O$ and 1 g of CH_3CSNH_2 were dissolved in 50 mL deionized water under magnetic stirring for 10 min. Subsequently, 0.3 g CTAB was added to the above mixed solution with vigorous magnetic stirring for 30 min. Then, the obtained solution was transferred into a 100 mL Teflon-lined stainless autoclave and heated at 180 °C for 24 h. The autoclave was cooled down to room temperature naturally. The precipitates were separated by centrifugation and purified by washing with ethanol and deionized water for several times. The black product was dried at 60 °C oven for 10 h. To explore the effect of CTAB concentration on the morphology of the final product and find the optimal CTAB concentration, the synthesis process of the other three samples is the same with the MoS_2 (0.3g, S3) except the initial addition of CTAB, which is 0g (S1), 0.1g (S2) and 0.5g (S4), respectively.

2.2. Characterization

The structure and purity of the obtained MoS_2 samples were characterized via X-ray diffraction using a Rigaku D/Max-1200X diffractometer with Cu Kα radiation operated at 30 kV and 100 mA. The diffraction angle (2θ) ranged of 5° to 70°. The surface micromorphology and nanostructures of the samples were analyzed by a Nova field emission scanning electronic microscope (FE-SEM) and transmission electron microscopy (TEM, ZEISS, LIBRA 200) operated at an accelerating voltage of 200 kV [13,14].

2.3. Fabrication and measurement of gas sensor

Fig. 1 displays a picture of the structure of NO_2 sensors fabricated on a ceramic substrate. Ag–Pd substrate was placed at the ceramic substrate of length 7 mm and thickness 13.2 mm, respectively. As shown in Fig. 2 (d), substrate thin film sensor was fabricated by dispersing the as–prepared MoS_2 powders with deionized water and glycol to form a homogenous mixture which was then coated on a ceramic substrate to develop a film of approximately 40 μm thickness. A protective layer consisting of 0.1 g ethyl cellulose solution in ethyl ester acetate was developed to improve sensor antipollution [15]. Finally, the thin-film sensor was dried in the air to remove unsolicited impurities for 48 h.

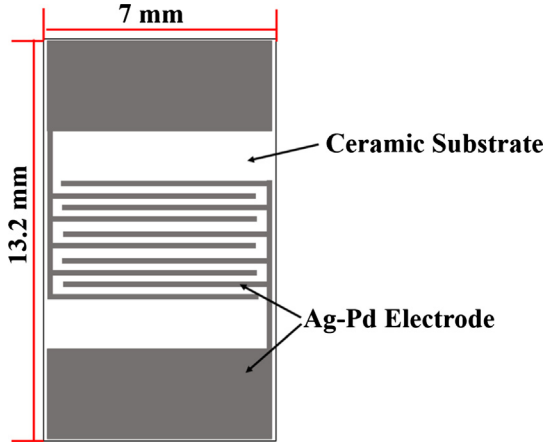

Fig. 1. Schematic diagram of sensor electrode substrates.

Gas-sensing properties towards NO_2 were measured using CGS–1TP (Chemical Gas Sensor–1 Temperature Pressure) intelligent gas-sensing analyzer system (Beijing Elite Tech Co., Ltd.), composed of gas–supply valves, vacuum chamber (24L), temperature controller (RT–500 °C), heating system, probe adjustment and data acquisition system, as shown in Fig. 2 (a). The magnified top–view of the operating stage is shown in Fig. 2(b). The temperature–controlling platform consists of two adjustable probes pressed on the sensor as electrical signal collectors (Fig. 2(c)). The as–prepared sensors were pre-heated for 30 min until they reached a stable resistance at working temperature. The known concentration of target gas was injected into the vacuum chamber by using a dynamic gas disruption system. The entire experiments were conducted at room temperature (about 20.0 ± 1.5 °C) and relative humidity level of 35% RH.

The sensor response in this work is calculated from the relation: $R = \triangle R/Ra = (Rg - Ra)/Ra \times 100\%$, where Ra and Rg are the resistances of the sensor in the air and target gas, respectively. Response and recovery time are defined as change in the resistances from Ra to [Ra–90% × (Ra − Rg)] for gas-in and [Ra + 90% × (Ra − Rg)] to gas–out, respectively [16].

3. Results and discussion

3.1. 3D MoS_2 nanostructures characterizations

Fig. 3a shows the X-ray diffraction patterns of the as-synthesized MoS_2 samples, which are utilized to identify the crystal structure and phase composition. All the diffraction peaks could be indexed to hexagonal MoS_2 (JCPDS card No. 37-1492, molybdenite) in spite of the deviation of (0 0 2) and (0 0 4) diffraction peaks. The shift of the (0 0 2) and (0 0 4) peaks is ascribed to the increased S–Mo–S interlayer distance. The expansion of S–Mo–S interlayer distance may be related to bending of the MoS_2 slabs, strain effects, defects involving folding of the layers [17]. During the synthesis process, the intercalation of the excess ammonium ions and the involvement of CTAB may also cause the expansion of S–Mo–S interlayer distance [18]. In addition, no diffraction peaks of any other impurities are observed, demonstrating that high purity MoS_2 samples are successfully synthesized via the facile hydrothermal process. It is worth noting that all the peaks are significantly broadened and low intensities, suggesting pronounced short-range order, poor crystallinity and sizes of coherent scattering domains within the nanoregime [19] or the nanoscale of the crystallites in different dimensions [20]. In Fig. 3b, the energy-dispersive X-ray spectrometer (EDS) is conducted on the S3. The EDS result clearly reveals that the sample consists of Mo and S without other elements. The chemical states of Mo and S in the flower-like MoS_2 nanospheres were confirmed via the high-resolution XPS spectra as shown in Fig. 4. In Fig. 4a, the XPS peaks at 232.3 and 229.1 eV are caused by the binding energy of Mo 3d 3/2 and Mo 3d 5/2, respectively, demonstrating the existing of Mo^{4+} in the flower-like MoS_2 nanospheres. In Fig. 4b, the XPS peaks at 163.2 and 162.0 eV are ascribed to the binding energy of S 2p 1/2 and S 2p 3/2 respectively, indicating the presence of S^{2-} in the MoS_2 nanospheres [21,22].

The morphologies and microstructures of MoS_2 nanospheres (S3) were investigated by SEM and TEM (Fig. 5). According to Fig. 5a, we can clearly see that the samples are composed of hierarchical flower-like spheres with an average diameter of 300 nm. From the magnified